Environmental Science & Technology

Article

Cite This: Environ. Sci. Technol. 2018, 52, 4592−4600

pubs.acs.org/est

# Probing the Differential Tissue Distribution and Bioaccumulation Behavior of Per- and Polyfluoroalkyl Substances of Varying Chain-Lengths, Isomeric Structures and Functional Groups in Crucian Carp

Yali Shi,[†] Robin Vestergren,[⊥,‡] Therese Haugdahl Nost,[§,#] Zhen Zhou,[∥] and Yaqi Cai*[,†]

[†]State Key Laboratory of Environmental Chemistry and Ecotoxicology, Research Center for Eco-Environmental Science, Chinese Academy of Sciences, Beijing, China

[‡]ACES, Stockholm University, Stockholm SE 10691, Sweden

[§]Department of Community Medicine, Faculty of Health Sciences, UiT − The Arctic University of Norway, 6050 Langnes, 9037 Tromsø, Norway

[∥]Key Laboratory of Optoelectronic Chemical Materials and Devices, Ministry of Education, School of Chemical and Environmental Engineering, Jianghan University, Wuhan, China

[⊥]IVL Swedish Environmental Research Institute, Stockholm, Sweden

[#]FRAM-High North Research Centre on Climate and the Environment, Norwegian Institute for Air Research, 9296 Tromsø, Norway

Supporting Information

**ABSTRACT:** Understanding the bioaccumulation mechanisms of per- and polyfluoroalkyl substances (PFASs) across different chain-lengths, isomers and functional groups represents a monumental scientific challenge with implications for chemical regulation. Here, we investigate how the differential tissue distribution and bioaccumulation behavior of 25 PFASs in crucian carp from two field sites impacted by point sources can provide information about the processes governing uptake, distribution and elimination of PFASs. Median tissue/blood ratios (TBRs) were consistently <1 for all PFASs and tissues except bile which displayed a distinct distribution pattern and enrichment of several perfluoroalkyl sulfonic acids. Transformation of concentration data into relative body burdens (RBBs) demonstrated that blood, gonads, and muscle together accounted for >90% of the amount of PFASs in the organism. Principal component analyses of TBRs and RBBs showed that the functional group was a relatively more important predictor of internal distribution than chain-length for PFASs. Whole body bioaccumulation factors (BAFs) for short-chain PFASs deviated from the positive relationship with hydrophobicity observed for longer-chain homologues. Overall, our results suggest that TBR, RBB, and BAF patterns were most consistent with protein binding mechanisms although partitioning to phospholipids may contribute to the accumulation of long-chain PFASs in specific tissues.

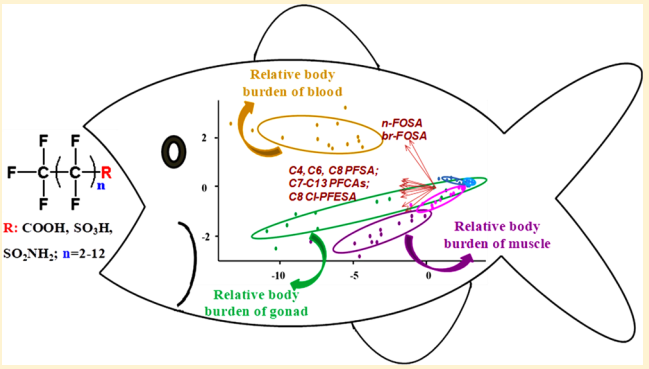


## INTRODUCTION

Per- and polyfluoroalkyl substances (PFASs) is the summary term for a broad class of anthropogenic chemicals that have been subject to intense research since 2001 when their global presence in humans and wild-life samples was first discovered.[1,2] Particular attention has been directed to the long-chain perfluoroalkanesulfonic acids (PFSAs, $C_nF_{2n+1}SO_3H$, $n \geq 6$) and perfluoroalkyl carboxylic acids (PFCAs, $C_nF_{2n+1}COOH$, $n \geq 7$) which are highly persistent, bioaccumulative and exert different forms of toxicity in animal models.[3,4] Due to their adverse environmental properties a series of actions have been taken to substitute long-chain PFASs and their respective precursors with shorter-chain homologues and an array of per- and polyfluoroalkyl ether compounds.[5−7] As many of these PFAS alternatives are structurally similar to the chemicals that they replace, scientists and regulators worldwide are calling for improved approaches to comprehensively assess the hazard profiles of PFASs.[8−10]

One of the major obstacles for effective management of PFASs is to determine whether or not they fulfill regulatory criteria for bioaccumulation potential (B) which has caused delays in regulatory decisions for substances such as perfluorooctanoate (PFOA).[11] For neutral hydrophobic chem-

Received: November 29, 2017
Revised: March 14, 2018
Accepted: March 21, 2018
Published: April 3, 2018




DOI: 10.1021/acs.est.7b06128
Environ. Sci. Technol. 2018, 52, 4592−4600

icals, the octanol−water partitioning coefficient ($K_{ow}$) is often used in chemical hazard assessment as surrogate for empirical bioconcentration/bioaccumulation factors (BCFs/BAFs).[12] As PFASs, unlike most traditional persistent organic pollutants, are not lipophilic the existing regulatory paradigm based on octanol−water partitioning cannot be used for this group of substances. Assessment of the B criteria for PFASs, therefore, relies on empirical measurements of BAFs/BCFs, biomagnification factors in fish or elimination rates in mammalian species[3,12,13] which are time-consuming to generate and often insufficient to cover interspecies variability in bioaccumulation potential.

In order to overcome this gap in chemical hazard characterization, significant research efforts are needed to understand the underlying mechanisms of PFAS bioaccumulation and develop mechanistic bioaccumulation models.[14−17] So far, two conceptually different hypotheses have been proposed to explain the bioaccumulation behavior of PFASs. One hypothesis stipulates that partitioning to phospholipid bilayers, which have a moderate affinity for PFASs,[15,18] has a major influence on the whole body bioaccumulation potential of PFASs in aquatic organisms.[15,18] The other hypothesis suggests that noncovalent interactions with various proteins (e.g., serum albumin, fatty acid binding proteins, and organic anion transporters (OATs)) are the most important mechanisms that govern the uptake, distribution and elimination of PFASs.[19] A central observation in the discussion of PFASs bioaccumulation mechanisms is the characteristic tissue distribution and to what extent it can be explained by the phospholipid partitioning and protein binding hypothesis, respectively.[14,15] Data on internal distribution of PFASs have, however, primarily been reported for linear long-chain PFCAs and PFSAs in a limited number of tissues.[20−28] For short-chain PFASs and branched isomers of perfluorooctanesulfonic acid (PFOS) and PFOA data on tissue distribution are scarce and/or display substantial inconsistencies between different studies and species.[29−32] For example, one study on human autopsy samples suggests that short-chain PFCAs have enrichment factors in some tissues (particularly brain tissue) that exceed those of long-chain PFASs by several orders of magnitude.[30] This finding is in stark contrast to the toxicokinetic studies in rodents which show that the apparent volume of distribution for short- and long-chain PFCAs are typically within a factor of 2.[31] The lack of conclusive data on tissue distribution for short-chain PFASs and branched isomers can partly be explained by the difficulties to accurately quantify these substances at background concentrations in biomonitoring studies. Controlled toxicokinetic studies, on the other hand, are usually performed only for single or a few substances at the same time making it difficult to compare distribution patterns for a wide range of PFASs with different chain-lengths, isomeric structures and functional groups. Comparing data from controlled dose studies with environmentally relevant exposure conditions may also be complicated by the difference in dose levels,[33] presence of precursor compounds[34] and the physiological conditions of the model species.[35,36]

In this study we investigate the distribution patterns for a wide range of PFASs with varying chain-lengths, isomeric structures and functional groups in multiple tissues of crucian carp to provide information about the underlying bioaccumulation mechanisms. By analyzing water and biota samples from two different freshwater systems impacted by point source emissions we were able to quantify 25 individual PFASs in whole blood, bile and 8 different organ tissues of crucian carp. The data sets were subsequently analyzed using multivariate statistics to identify differential accumulation patterns among different tissues and PFASs.

## MATERIALS AND METHODS

**Model Species and Sample Collection.** Crucian carp (*Carassius carassius*) was selected as a model species due to its stationary nature and widespread distribution in fresh water systems throughout China. Two different fresh water systems in China with exceptionally high levels of PFASs, Tangxun lake and Xiaoqing river, were chosen for this study to achieve a high detection frequency for a large number of analytes. These two sampling locations are hereafter referred to as TL and XR respectively. TL is a shallow lake with a surface area of 32 $km^2$ located in Hubei province, which receives municipal and industrial wastewater with suspected input from perfluorooctyl and perfluorobutyl sulfonyl fluoride (POSF/PBSF) production.[37] XR, located in Shandong province, is a 216 km long river that runs parallel to the Yellow river in a SW−NE orientation. XR receives industrial discharges from one of the world's largest production facilities of fluoropolymers including polytetrafluoroethylene (PTFE), polyvinylidene fluoride (PVDF), fluorinated ethylene propylene (FEP) and hexafluoropropylene (HFP).[38]

In July 2014 a total of 43 crucian carp were collected from XR ($n$ = 30) and TL ($n$ = 13). All fish were alive during sampling and 2−5 mL whole blood samples ($n$ = 43) were drawn using syringe, rinsed with a heparin sodium solution, and then transferred to a BD Vacutainer tube (Becton Dickinson Vacutainer System, UK) with EDTA. The fish were subsequently dissected in the field to extract liver ($n$ = 43), kidney ($n$ = 43), brain ($n$ = 43), heart ($n$ = 42), swim bladder ($n$ = 43), gill ($n$ = 43), gonad ($n$ = 43) and muscle samples ($n$ = 43), which were cleaned using milli-Q water to remove excess blood, and then homogenized. In addition, sufficient volumes of bile could be collected from 29 individuals. All samples were stored in an ice-box and transported to the laboratory after collection as soon as possible where they were kept at −20 °C until chemical analysis. The length, weight, and sex of the fish were recorded along with the weight of all individual tissues except blood, and bile (Supporting Information (SI) Table S1). One liter surface water samples from TL ($n$ = 3) and XR ($n$ = 2) were collected at approximately 1 m depth in parallel with the fish samples using precleaned polypropylene beakers.

**Target Analytes and Terminology.** The target analytes for this study included linear (n-) perfluorobutanoic acid (PFBA), perfluoropentanoic acid (PFPeA), perfluorohexanoic acid (PFHxA), perfluoroheptanoic acid (PFHpA), PFOA, perfluorononaoic acid (PFNA), perfluorodecanoic acid (PFDA), perfluoroundecanoic acid (PFUnDA), perfluorododecanoic acid (PFDoDA), perfluorotridecanoic acid (PFTrDA), perfluorotetradecanoic acid (PFTeDA), perfluorobutanesulfonic acid (PFBS), perfluorohexanesulfonic acid (PFHxS), PFOS, linear perfluorooctane sulfomamide (n-FOSA), eight carbon chlorinated polyfluoroalkane ether sulfonic acid (C8 Cl-PFESA), branched isomers of PFOA (iso-, 5m-, 4m-, and 3m-), PFOS (iso- 1m-, 4$m$/3m-, and 5m-) and sum of branched isomers of FOSA (br-FOSA). For br-FOSA we reported the sum of isomers due to the lack of individual isomer standards. It should be noted that the concentrations of n-PFOS and C8 Cl-PFESA (referred to by its trade name F-53B) have already been reported in our previous



DOI: 10.1021/acs.est.7b06128
Environ. Sci. Technol. 2018, 52, 4592−4600

paper,[39] but were included in the statistical evaluation of this study. Throughout the manuscript, we often refer to homologues of PFCAs and PFSAs by their number of perfluorinated carbon atoms (e.g., PFBA as C3 PFCA and PFBS as C4 PFSA).

**Sample Treatment.** A complete description of reagents and standards is provided in the Supporting Information (SI). For surface water samples, the preconcentration and cleanup were similar to methods used in our previous studies.[37,38] In brief, 200 mL of water, prefiltered through a 0.7 $\mu$m glass fiber filter membrane, was spiked with 2 ng of internal standard (MPFCA-MXB) and then loaded onto an Oasis WAX single-use cartridge (6 cc/150 mg), which was preconditioned using 4 mL of 0.1% ammonium hydroxide (in methanol), 4 mL of methanol, and 4 mL of ultrapure water at a rate of 1 drop/s. The cartridges were subsequently washed using 4 mL of buffer solution (25 mmol/L acetic acid/ammonium acetate, pH 4) and 8 mL of ultrapure water and centrifuged for 10 min at 3000 rpm to remove the residual water. Finally, the target compounds were eluted using 4 mL of methanol and 4 mL of 0.1% ammonium hydroxide (in methanol), which was subsequently concentrated to 1 mL under nitrogen gas prior to injection. All tissue samples were pretreated using two different extraction methods: alkaline digestion and ion-pairing liquid−liquid extraction, which have been described in detail previously.[39] Muscle samples were homogenized and freeze-dried under vacuum, followed by alkaline digestion and methanol extraction. In this procedure 0.2 g freeze-dried muscle sample spiked with 2 ng of internal standards was sonicated for 30 min in 10 mL of 10 mmol/L KOH methanol solution at 60 °C, followed by shaking at 250 rpm for 16 h. Blood, bile and organ samples were extracted using ion-paring liquid−liquid method. In detail, 0.2−0.5 g of each samples were spiked with 2 ng of internal standards, 2 mL of $NaHCO_3$/$Na_2CO_3$ buffer solution (pH 10) and 1 mL of TBA solution for 0.5 h, and then extracted using 5 mL MTBE for three times by shaking at 250 rpm for 20 min. The supernatant was transferred, combined and then concentrated to 1 mL under nitrogen. Concentrated extracts of each sample were diluted to about 50 mL using ultrapure water and loaded onto a WAX cartridge following the procedure for water samples.

**Instrumental Analysis.** Instrumental analysis was performed using high performance liquid chromatography (HPLC) with a dual pump and autosampler (Ultimate 3000, ThermoFisher Scientific), coupled to electrospray ionization tandem mass spectrometry (ESI-MS/MS, API 4500, Applied Biosystems/MDS SCIEX), with separation on an Ascentis Express F5 PFP Column (2.7 $\mu$m, 90 Å, 2.1 mm × 100 mm, Sigma-Aldrich). The mobile phase was a mixture of methanol (eluent A) and 20 mM ammonium hydroxide/20 mM formic acid in water (eluent B). The solvent gradient started at 90% B, then ramped to 40% B by 1.0 min and held for 2 min, decreased to 12% B by 14 min, 0% B by 14.5 min, returned to initial conditions by 14.6 min and held for 6.4 min. The flow rate was held at 0.25 mL/min.

**Quality Assurance.** All laboratory consumables, solvents, and dissection tools were checked for contamination, and one procedural blank sample was conducted for every ten samples. Field blanks included polypropylene bottles filled with milli-Q water and aluminum wrappers which were opened in the field. However, all procedural, field, and solvent injection blanks were consistently below instrumental detection limits. Instrumental drift was monitored by injecting a calibration standard for every 10 sample injections and a new calibration curve was constructed if a deviation of more than ±20% from its initial value was observed. Spike-recovery experiments were conducted by adding 2 ng of the native compounds to crucian carp tissue samples ($n$ = 4) purchased on a Beijing market which had substantially lower concentrations of PFASs. In brief, the mean recoveries for all analytes and tissues were within 70−120%, except PFDA, PFUnDA, PFTrDA, and PFTeDA which had recoveries below 70% in some tissues, with a relative standard deviation of <20% (SI Table S4). Method quantification limits (MLQs) were calculated using a signal-to-noise ratio of 10 from a nine-point calibration curve ($r^2$ > 0.99). MLQs ranged 0.01−0.20 ng/L in water and 0.002−0.66 ng/g in tissue samples (SI Table S4). Method detection limits (MDLs) were calculated using MLQs divided by 3. High resolution mass spectrometry (HRMS) with an Orbitrap Fusion MS system (Thermo Fisher Scientific, Waltham, MA) was employed to confirm the identity of PFBA and PFPeA, which only have one product ion in MS/MS detection. Details regarding HRMS parameters and chromatograms of PFBA and PFPeA in tissue samples are provided in the SI.

**Data analysis.** The propensity of PFASs to leave the bloodstream and distribute to different tissues was assessed by calculating tissue/blood ratios (TBRs; unitless) on a wet weight concentration basis. To evaluate the contribution of specific tissues to the whole body bioaccumulation potential, a relative body burden (RBB; %) was calculated according to the following equation:

$$\mathrm{RBB}_{\mathrm{tissue}} = 100 \times \frac{C_{\mathrm{tissue}} \times m_{\mathrm{tissue}}}{\sum_{n=1}^{i} C_{\mathrm{tissue},n} \times m_{\mathrm{tissue},n}}$$

Where $C_{\mathrm{tissue}}$ is the PFAS concentration in a particular tissue (ng/g ww) and $m_{\mathrm{tissue}}$ is the weight of the tissue (g). Tissue-specific and whole body bioaccumulation factors ($\mathrm{BAF}_{\mathrm{tissue}}$ and $\mathrm{BAF}_{\mathrm{whole\ body}}$; L/kg) were calculated by the following equations:

$$\mathrm{BAF}_{\mathrm{tissue}} = \frac{C_{\mathrm{tissue}}}{C_{\mathrm{water}}}$$

$$\mathrm{BAF}_{\mathrm{wholebody}} = \frac{\sum_{n=1}^{i} C_{\mathrm{tissue},n} \times f_{\mathrm{tissue},n}}{C_{\mathrm{water}}}$$

Where $f_{\mathrm{tissue}}$ (unitless) is the mass fraction of tissue relative to the total body weight and $C_{\mathrm{water}}$ is the surface water concentration of PFASs. All calculations were performed for individual fish using measured concentrations for PFASs and tissue weights from post mortem examination (SI Table S1). Since blood and muscle weights could not be accurately determined $f_{\mathrm{tissue}}$ values were set to 0.045 and 0.5 respectively based on literature values.[40] The carcass was assumed to have half PFAS concentrations of muscle in $\mathrm{BAF}_{\mathrm{whole\ body}}$ calculations.[41]

**Statistical Analysis.** The statistical analyses included measurement data from 286 and 129 samples from XR and TL respectively. Statistical analyses were executed using the software R, ver. 3.0.0 considering a statistical significance threshold of $p$ < 0.05. Summary statistics for concentrations, TBRs and RBBs were calculated for PFASs with detection frequencies >80% in all tissues using MDL/2 as a substitute for nondetects. BAFs were calculated for PFASs with detectable concentrations in surface water and detection frequencies >80% in at least one tissue using MDL/2 as a substitute for


DOI: 10.1021/acs.est.7b06128
Environ. Sci. Technol. 2018, 52, 4592−4600

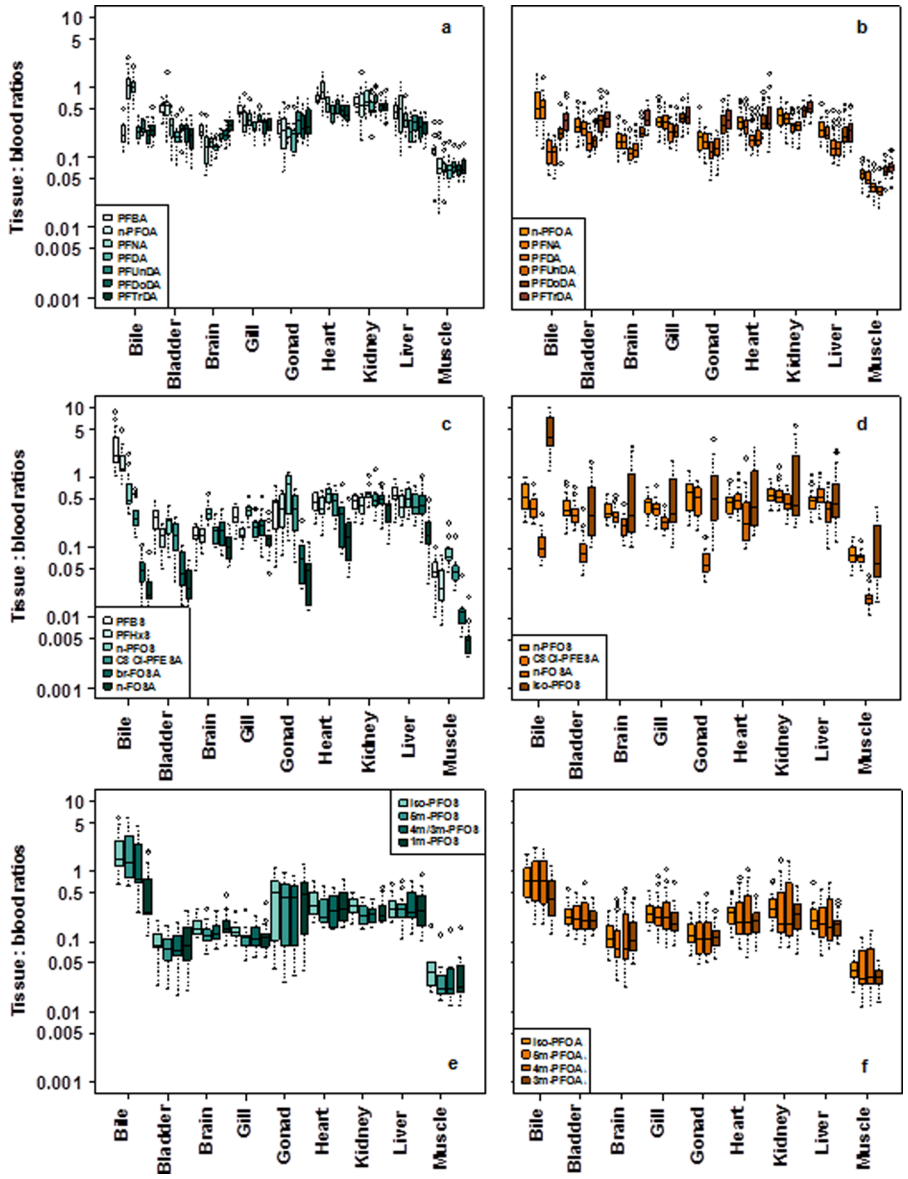


**Figure 1.** Box-whisker plots of TBRs for PFASs in TL (blue) and XR (orange). Data with <80% detected concentrations in all tissues were excluded. Boxes indicate 25th, 50th, and 75th percentiles and whiskers indicate 5th and 95th percentiles. Extreme values in the data sets are indicated as circles. a and b: C3, C7−C13 PFCAs; c and d: PFBS, PFHxS, n-PFOS, C8 Cl-PFESA, br-FOSA, and n-FOSA; e and f: br-PFOS and br-PFOA isomers.

nondetects. Wilcoxon rank sum test was used to test for differences in blood concentrations between male and female fish. Principal component analysis was carried out for TBRs and RBBs including PFASs that were detected in >80% of the samples from all tissues in each location.

## RESULTS AND DISCUSSION

**Concentrations of PFASs in Water and Tissue Samples.** The detection frequency and concentrations of analytes displayed large variation between the locations and sample matrices reflecting the composition of emission sources and partitioning behavior of PFASs. In surface water, C3−C10 PFCAs; C4, C6, and C8 PFSAs; n-FOSA; and C8 Cl-PFESA were detected in 100% of the samples from TL and XR. TL water samples also had detectable concentrations of br-FOSA and all individual branched isomers of PFOA and PFOS. In XR water samples all individual isomers of PFOA were detected. C11−C13 PFCAs were consistently < MDL in water samples from both locations. Median ∑PFAS concentrations in water samples from TL and XR were similar (30.0 μg/L and 25.9 μg/L respectively) although the composition of individual PFASs varied greatly. PFBA (16.5 μg/L) and PFBS (7.97 μg/L) displayed the highest median concentrations in TL, whereas the sum of PFOA isomers (22.5 μg/L), PFHxA (3.80 μg/L) and PFHpA (2.18 μg/L) dominated in XR samples. Detection frequencies and concentrations in fish samples also varied greatly for the different PFASs. In XR, C3, C7−C12 n-PFCAs, and all branched isomers of PFOA, n-PFOS, C8 Cl-PFESA, and n-FOSA were detected in >80% of the samples from all tissues. In TL, C7−C12 n-PFCAs and iso-PFOA, PFBS, PFHxS, all isomers of PFOS, C8 Cl-PFESA, n-FOSA, and br-FOSA were detected in >80% of the samples from all tissues. No consistent gender differences in concentrations of PFASs in blood were observed for TL or XR samples (SI Table S5) and concentrations were therefore presented together.



DOI: 10.1021/acs.est.7b06128
Environ. Sci. Technol. 2018, 52, 4592−4600

As expected from the surface water measurements, PFAS profiles in crucian carp blood samples from TL and XR were distinct from each other (SI Figure S2a−d). Long-chain PFASs were generally found in the highest concentrations in blood samples from both TL and XR which is explained by the positive relationship between bioaccumulation factor and perfluoroalkyl chain-length.[3,42] However, the data sets from TL and XR displayed several interesting anomalies compared with the majority of biomonitoring data on aquatic biota.[43] First, it should be noted that XR samples displayed a rather unique homologue pattern of PFCAs with concentrations of PFOA exceeding those of PFNA, PFDA, and PFUnDA by 1−2 orders of magnitude. In TL blood samples, the levels of PFBA were comparable to or exceeded those of long-chain PFCAs which is in stark contrast to the majority of previous studies.[43] Blood samples from TL also displayed high concentrations of PFBS which was the most abundant PFAS after PFOS and FOSA isomers. The unique PFAS profiles in fish blood samples from both TL and XR can be explained by the proximity to point sources reflecting ongoing emissions from POSF/PBSF- and fluoropolymer manufacture at TL and XR, respectively. The significant contribution of short-chain PFASs, particularly in TL, indicates that these replacement substances are produced/used in parallel with long-chain homologues although their emission sources are not well documented.[37,38] While the homologue patterns of PFCAs displayed substantial differences between the two locations, isomer profiles of PFOA were comparable with median values of ∑br-PFOA at 15.0% and 16.4% in TL and XR respectively. Furthermore, the profile of individual branched PFOA isomers (n- > iso- ≥ 3m- >5m- ≥ 4m-) was identical in both locations (SI Figure S2b). PFOS isomers displayed a higher proportion of ∑br-PFOS in TL (21.2%) compared to XR (10.5%) but there was no difference in the relative occurrence of individual isomers (n- >iso- > 4*m*/3m- > 5m- > 1m-).

**Tissue Distribution of PFASs.** The internal distribution of PFASs is depicted as box-whisker plots of TBRs in Figure 1. Median TBRs for PFCAs were consistently <1 in all tissues except for n-PFOA in bile of TL (Figure 1a and b). After bile, the highest TBRs for PFCAs were observed in heart, kidney and liver for TL and gills, gonad, bladder, heart, kidney, and liver for XR. TBRs for PFCAs were consistently lowest in muscle tissue in both TL and XR. A weak negative trend in TBRs with increasing chain-length was observed from C3 to C9 PFCAs in the majority of tissues. However, in some tissues TBRs increased for C10 to C12 PFCAs resulting in a U-shaped pattern with increasing chain-length. This U-shaped trend was observed for the majority of tissues in XR, but only in brain and gonad from TL. All branched isomers of PFOA, except iso-PFOA in bile, displayed lower median TBRs compared to n-PFOA (Figure 1f). TBRs for PFSAs, C8 Cl-PFESA and FOSAs displayed considerable variability within the different tissues and particularly in bile (Figure 1c and d). Except for the strong enrichment of PFBS and PFHxS in bile, the highest median TBRs for PFSAs and C8 Cl-PFESA were observed in gonad, heart, kidney and liver. FOSAs displayed considerably lower TBRs than PFSAs and C8 Cl-PFESA for all tissues with distribution primarily to heart, kidney and liver (Figure 1c). PCA plots revealed a contrasting variation between bile, kidney, and muscle versus all other tissues in both TL and XR data sets (SI Figure S3). For TL samples PFBS, PFHxS, iso-PFOS, 4*m*/3m-PFOS and 5m-PFOS were associated with bile whereas long-chain PFCAs were associated with kidney. For XR samples, iso-PFOS and br-PFOA isomers were associated with bile whereas the linear long-chain PFCAs were associated with the other tissues.

The most pronounced differences in TBRs were observed between the classes of PFASs while the differences between homologues were relatively small, demonstrating that the headgroup of PFASs is a relatively more important predictor of the internal distribution than chain-length. Previous studies have shown that FOSA distributes primarily to the red blood cell fraction due to less favorable electrostatic interactions with serum albumin compared to the fully protonated PFCAs and PFSAs.[44−46] Based on the consistently higher TBRs of PFCAs and PFSAs compared to FOSA the acid functionality also appears to increase the distribution of PFASs to other tissues than blood. Perfluoroalkyl carboxylic and sulfonic acids of varying chain-lengths, isomeric structures or inclusion of heteroatoms displayed fairly consistent TBRs for the majority of tissues (within a factor of 2 for the majority of PFASs). The lack of strong enrichment in tissues is consistent with the majority of toxicokinetic studies showing that PFCAs of varying chain length are primarily distributed to the extracellular space of tissues.[31] Uptake to the intercellular space of tissues or partitioning to phospholipid bilayers may, however, explain the subtle differences in TBRs with perfluoroalkyl chain-length resulting in the U-shaped trend for some tissues. For example, the slightly higher TBRs of PFBA and PFBS compared to C8 homologues may be explained by the lower affinity for serum albumin,[19,47] allowing these substances to be more readily available for transfer to tissues and elimination from the organism. The relatively high TBRs for PFDoDA and PFTrDA in brain, gonad, and swim bladder may, on the other hand, reflect the chain-length dependence in membrane-water partitioning of PFCAs and high phospholipid content of these tissues.[19,48] Similar trends with a preferential distribution of longer chain PFCAs to brain tissue have also been reported in sea gulls[28] and polar bears.[20] TBRs in bile varied greatly for PFASs with different functional group and displayed no clear trend with perfluoroalkyl chain-length for sulfonic acids or carboxylic acids. TBRs in bile were also isomer-specific with all branched isomers of PFOA and PFOS (except 1m-PFOS) being more efficiently transferred to bile compared to the linear isomer. The contrasting TBR pattern in bile suggests that the distribution mechanism is distinct from the majority of tissues which may be explained by active transport mediated by specific proteins.[14,49]

**Relative Body Burdens of PFASs.** Blood, gonads and muscle contributed to >90% of the total body burden although the relative importance of these three tissues displayed some variation for the different PFASs and locations (SI Figure S4). The highest median RBBs in gonads were observed for PFSAs and particularly iso-PFOS (42.5%), n-PFOS (37.9%), 5m-PFOS (35.7%), 4*m*/3m-PFOS (38.6%), and 1m-PFOS (35.2%) in TL. The higher RBBs in gonads for TL can be explained by a higher gonad somatic index compared to XR (SI Table S1) which results in a larger contribution of this tissue to the total body burden. For PFCAs, blood and muscle were relatively more important as storage depots with median RBBs ranging 33−50% and 24−35%, respectively, in both TL and XR. PCA plots displayed in Figure 2a and b illustrate a large variation in gonads, blood and muscle compared to the other tissues for both TL and XR. Br-FOSAs and n-FOSA were associated with blood while all other compounds were correlated with gonads and muscle.


DOI: 10.1021/acs.est.7b06128
Environ. Sci. Technol. 2018, 52, 4592−4600

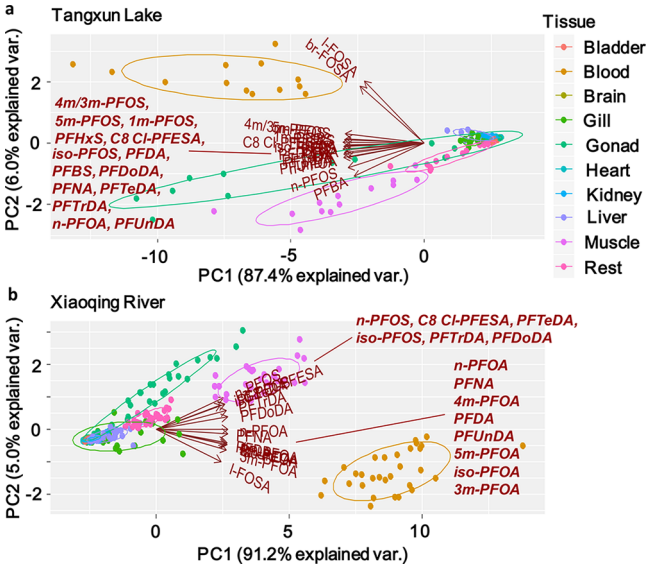


**Figure 2.** PCA plots for RBBs in TL (a) and XR (b). Due to the strong correlations of several PFASs separate labels are used to list the compounds for each cluster.

In previous papers discussing the importance of protein binding versus phospholipid partitioning the tissue distribution has primarily been discussed on the basis of concentration ratios (referred to as TBRs in this paper) leading to a focus on kidney and liver as the main target organs.[14,15] By evaluation of RBBs it is evident that blood, gonads and muscle individually has a larger impact on the whole body bioaccumulation potential than all other tissues combined. In the case of muscle tissue, the high RBBs were due to the large mass fraction of this tissue whereas the high RBBs in gonads were due to a combination of relatively large mass fractions (especially in TL) and high affinity of PFASs (especially PFSAs) in this tissue. Regardless if the RBBs were driven by the concentration of PFASs or mass fraction, the sorption mechanisms of these tissues play a crucial role for determining the whole body bioaccumulation potential. In blood, it is widely accepted that sorption to serum albumin is the main mechanism for accumulation of PFCAs and PFSAs.[14,15] Given that muscle tissue holds a comparable mass fraction of albumin as blood[14] the similar RBBs of PFASs in muscle and blood may be largely explained by sorption to extracellular albumin. Such a mechanism would also be consistent with the low TBRs of PFASs in muscle as the concentration of extracellular albumin is more than 10 times lower than that in blood.[14] In gonads, the large interindividual variability of RBBs and more pronounced compound-specific RBBs indicate that specific binding (e.g., binding to fatty acid binding proteins) or partitioning to phospholipids also contributes to the sorption capacity. In our previous paper, we hypothesized that the high phospholipid content of gonads contributes to the sorption capacity of n-PFOS and Cl-PFESA in this tissue.[39] As phospholipid partitioning is expected to increase with perfluoroalkyl chain-length[15,18] this mechanism could potentially explain the slight increase in TBRs and RBBs for C10−C12 PFCAs (Figure 1 and SI Figure S4). At the same time, PFSAs and particularly branched isomers of PFOS displayed higher RBBs compared to long-chain PFCAs in gonads suggesting that electrostatic interactions and sterical effects, in addition to hydrophobicity, are important for determining the sorption capacity of gonad tissue.

**Tissue-Specific and Whole Body BAFs.** PFCAs and PFSAs with six or more perfluorinated carbons displayed a positive trend in BAFs with increasing chain-length and distinct differences for PFASs with different functional groups (sulfonic acid > sulfonamide > carboxylic acid). Branched isomers of PFOS and PFOA had consistently lower BAFs compared to the linear isomer while the inclusion of an ether bond and/or terminal chlorine leads to a higher BAF for C8 Cl-PFESA compared to n-PFOS (Figure 3). For short-chain PFASs, there was no apparent relationship between BAF and perfluoroalkyl chain-length. Although PFHxA displayed a lower BAF compared to PFHpA, the difference in BAF from an additional $CF_2$ unit was lower compared to C7 to C10 PFCAs. Furthermore, median BAFs of PFBA were higher than those of PFPeA, PFHxA, and PFHpA which clearly deviated from the trend of long-chain PFCAs. Tissue-specific BAFs displayed

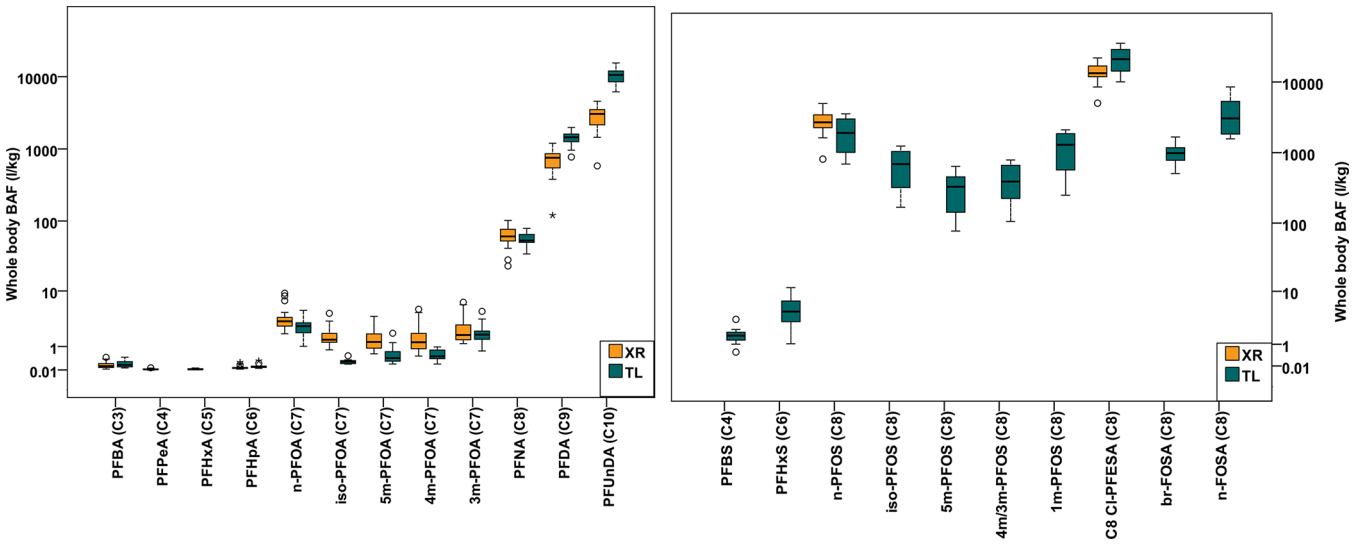


**Figure 3.** Whole body BAFs with chain-length and isomers for TL (blue) and XR (orange). Boxes indicate 25th, 50th, and 75th percentiles and whiskers indicate 5th and 95th percentiles. Extreme values are indicated as circles.



DOI: 10.1021/acs.est.7b06128
Environ. Sci. Technol. 2018, 52, 4592−4600

similar trends with respect to functional group, chain-length and isomers as whole body BAFs although the absolute values varied among the tissues (SI Figures S5−S13).

The lack of a positive association between chain-length and BAFs for short-chain PFASs represents an interesting observation for understanding the relative importance of different bioaccumulation mechanisms.[15] According to the phospholipid partitioning mechanism, whole body BAFs are expected to be proportional to log $K_{ow}$ values from which phospholipid membrane partition coefficients are derived. As estimated log $K_{ow}$ values for PFASs display a continuous positive association with chain-length[50] the phospholipid partitioning may be a plausible mechanism to explain the trend in BAFs of long-chain PFASs.[15] However, when extending the data set to include shorter-chain PFASs it becomes apparent that the phospholipid partitioning cannot readily explain the trend of whole body BAFs for short-chain PFASs. Considering the relatively small differences in TBRs and RBBs between homologous PFCAs and PFSAs respectively (see previous sections), the diverging trend in BAFs of short-chain PFASs also cannot be explained by a fundamentally different sorption mechanism compared to long-chain PFASs. Thus, phospholipid partitioning does not appear to be a valid mechanism to explain the accumulation and distribution of PFASs across a wide range of chain-lengths. Evaluating the chain-length patterns with respect to the protein sorption mechanism is more complicated as the whole body BAFs will be the net result of several different interactions with specific transporter proteins,[51,52] fatty acid binding proteins[53,54] and serum albumin.[55−59] In addition to this complexity, the protein sorption coefficients for serum albumin display rather inconsistent chain-length patterns and vary more than 2 orders of magnitude for the same compound between different studies.[57−60] Thus, it is not possible to evaluate weather the observed chain-length patterns in BAFs are consistent with protein sorption mechanisms or not.

When comparing absolute BAF values reported in fish from TL and XR to those reported in literature there is some variability between different study sites and species which may be attributed to differences in physiology, exposure conditions and environmental factors.[21,27,42] Increasing organism size is generally associated with slower depuration rates and/or higher trophic status of the organism which may lead to an increase in the bioaccumulation potential for organic contaminants.[12] Higher concentrations of PFASs may, on the other hand, lead to more rapid depuration rates in aquatic organisms and result in a lower bioaccumulation potential at higher exposures.[61] Although the slightly lower median BAFs of PFOS in TL than XR could potentially be explained by the higher exposure concentrations there was no difference in BAFs for other PFASs (e.g., PFOA) that displayed large differences in concentrations (SI Figure S2). Clearly, other factors such as coexposure to precursors, variable concentrations of particulate and dissolved organic carbon and deviation from the steady-state assumption may also impact the absolute BAF values in different directions.

**Implications for Understanding Bioaccumulation of PFASs and Future Directions.** In this paper we present the most comprehensive study on PFAS bioaccumulation and tissue distribution to our knowledge (415 samples for 10 tissues and 25 analytes). Collectively, the observed trends in TBRs, RBBs, and BAFs were most consistent with specific protein interactions as the governing mechanism for uptake and accumulation of PFASs although phospholipid partitioning may contribute to the accumulation of long-chain PFASs in specific tissues. Nevertheless, there are still many uncertainties related to interpreting the trends in tissue distribution data and building mechanistic models. As noted previously by Ng and Hungerbuehler[14,15] improved understanding of the partitioning to phospholipids and protein sorption behavior for a wider range of PFASs under biologically relevant conditions is urgently needed. Combining measurements of PFASs with a biochemical characterization of tissue composition is another research priority that would allow improved statistical evaluation of the large interindividual variability in TBRs and RBBs in different tissues. Such data would also be valuable input for mechanistic models which typically rely on a mix of tissue composition data from different organisms including data from rodents to parametrize a fish model.[19]

The significant contribution of short-chain homologues to ∑PFAS concentrations, particularly in TL samples, demonstrates the need for a better understanding of the uptake and accumulation of these substances. Although the current study corroborates previous assumptions that these substances are not bioaccumulative according to regulatory criteria[3] and demonstrates that short- and long-chain PFCAs and PFSAs have a similar internal distribution in fish, the high mobility, and bioavailability in combination with the proximity of emission sources lead to relatively high levels in fish tissues. Considering that emissions of short-chain PFASs are expected to increase globally[7,8] these measurements from point source areas may be taken as early warnings of a poorly reversible global contamination issue.[11] It should also be noted that little is known about the bioaccumulation potential of short-chain PFASs with other functional groups and if biomagnification can occur in air-breathing organisms. We, therefore, strongly encourage further mechanistic bioaccumulation/biomagnification studies on short-chain PFASs to support a sustainable management of these substances.

## ■ ASSOCIATED CONTENT

### Supporting Information

The Supporting Information is available free of charge on the ACS Publications website at DOI: 10.1021/acs.est.7b06128.

Additional information regarding chemicals and reagents, instrumental analysis for confirmation of PFBA and PFPeA and other materials are shown in Table S1−S5 and Figure S1−S13 (PDF)

## ■ AUTHOR INFORMATION


### Corresponding Author

*Phone: +86 (10) 62849239; fax: +86 (10) 62849182; e-mail: caiyaqi@rcees.ac.cn.

### ORCID

Yali Shi: 0000-0001-9946-1525

Yaqi Cai: 0000-0002-2805-5535


### Notes

The authors declare no competing financial interest.

## ■ ACKNOWLEDGMENTS

This work was jointly supported by the National Natural Science Foundation of China (No. 21722705, 21537004, 21677154, 21777182), the Strategic Priority Research Program



DOI: 10.1021/acs.est.7b06128
Environ. Sci. Technol. 2018, 52, 4592−4600

of the Chinese Academy of Sciences (XDB14010201) and the Swedish research council Formas (Grant No. 2014-514).

## REFERENCES

(1) Giesy, J. P.; Kannan, K. Global Distribution of perfluorooctane sulfonate in wildlife. *Environ. Sci. Technol.* **2001**, *35* (7), 1339−1342.
(2) Hansen, K. J.; Clemen, L. A.; Ellefson, M. E.; Johnson, H. O. Compound-specific, quantitative characterization of organic fluorochemicals in biological matrices. *Environ. Sci. Technol.* **2001**, *35* (4), 766−770.
(3) Conder, J. M.; Hoke, R. A.; Wolf, W. d.; Russell, M. H.; Buck, R. C. Are PFCAs bioaccumulative? A critical review and comparison with regulatory criteria and persistent lipophilic compounds. *Environ. Sci. Technol.* **2008**, *42* (4), 995−1003.
(4) *Toxicological Effects of Perfluoroalkyl and Polyfluoroalkyl Substances*; DeWitt, J. C.; Ed.; Humana press, 2015.
(5) 3M Company: Voluntary use and exposure information profile for perfluorooctanoic acid and salts. Submission to USEPA, June 8, 2000. *USEPA Administrative Record AR226−0595*.
(6) U.S. Environmental Protection Agency, 2010/15 PFOA Stewardship Program. http://www.epa.gov/opptintr/pfoa/pubs/pfoastewardship.html 2006.
(7) Wang, Z.; Cousins, I. T.; Scheringer, M.; Hungerbühler, K. Fluorinated alternatives to long-chain perfluoroalkyl carboxylic acids (PFCAs), perfluoroalkane sulfonic acids (PFSAs) and their potential precursors. *Environ. Int.* **2013**, *60*, 242−248.
(8) Wang, Z.; Cousins, I. T.; Scheringer, M.; Hungerbuehler, K. Hazard assessment of fluorinated alternatives to long-chain perfluoroalkyl acids (PFAAs) and their precursors: status quo, ongoing challenges and possible solutions. *Environ. Int.* **2015**, *75*, 172−179.
(9) Blum, A.; Balan, S. A.; Scheringer, M.; Trier, X.; Goldenman, G.; Cousins, I. T.; Diamond, M.; Fletcher, T.; Higgins, C.; Lindeman, A. E.; Peaslee, G.; de Voogt, P.; Wang, Z.; Weber, R. The Madrid statement on poly- and perfluoroalkyl substances (PFASs). *Environ. Health. Persp.* **2015**, *123* (5), A107−111.
(10) Scheringer, M.; Trier, X.; Cousins, I. T.; De Voogt, P.; Fletcher, T.; Wang, Z.; Webster, T. F. Helsingor statement on poly- and perfluorinated alkyl substances (PFASs). *Chemosphere* **2014**, *114*, 337−339.
(11) Cousins, I. T.; Vestergren, R.; Wang, Z.; Scheringer, M.; McLachlan, M. S. The precautionary principle and chemicals management: The example of perfluoroalkyl acids in groundwater. *Environ. Int.* **2016**, *94*, 331−340.
(12) Arnot, J. A.; Gobas, F. A. P. C. A review of bioconcentration factor (BCF) and bioaccumulation factor (BAF) assessments for organic chemicals in aquatic organisms. *Environ. Rev.* **2006**, *14* (4), 257−297.
(13) Goss, K. U.; Brown, T. N.; Endo, S. Elimination half-life as a metric for the bioaccumulation potential of chemicals in aquatic and terrestrial food chains. *Environ. Toxicol. Chem.* **2013**, *32* (7), 1663−1671.
(14) Ng, C. A.; Hungerbuhler, K. Bioaccumulation of perfluorinated alkyl acids: observations and models. *Environ. Sci. Technol.* **2014**, *48* (9), 4637−4648.
(15) Armitage, J. M.; Arnot, J. A.; Wania, F.; Mackay, D. Development and evaluation of a mechanistic bioconcentration model for ionogenic organic chemicals in fish. *Environ. Toxicol. Chem.* **2013**, *32* (1), 115−128.
(16) Cheng, W.; Ng, C. A. A Permeability-limited physiologically based pharmacokinetic (PBPK) model for perfluorooctanoic acid (PFOA) in male rats. *Environ. Sci. Technol.* **2017**, *51* (17), 9930−9939.
(17) Armitage, J. M.; Erickson, R. J.; Luckenbach, T.; Ng, C. A.; Prosser, R. S.; Arnot, J. A.; Schirmer, K.; Nichols, J. W. Assessing the bioaccumulation potential of ionizable organic compounds: current knowledge and research priorities. *Environ. Toxicol. Chem.* **2017**, *36* (4), 882−897.
(18) Armitage, J. M.; Arnot, J. A.; Wania, F. Potential role of phospholipids in determining the internal tissue distribution of perfluoroalkyl acids in biota. *Environ. Sci. Technol.* **2012**, *46* (22), 12285−12286.
(19) Ng, C. A.; Hungerbuhler, K. Bioconcentration of perfluorinated alkyl acids: how important is specific binding? *Environ. Sci. Technol.* **2013**, *47* (13), 7214−7223.
(20) Greaves, A. K.; Letcher, R. J.; Sonne, C.; Dietz, R.; Born, E. W. Tissue-specific concentrations and patterns of perfluoroalkyl carboxylates and sulfonates in East greenland polar bears. *Environ. Sci. Technol.* **2012**, *46* (21), 11575−11583.
(21) Martin, J. W.; Mabury, S. A.; Solomon, K. R.; Muir, D. C. Bioconcentration and tissue distribution of perfluorinated acids in rainbow trout (Oncorhynchus mykiss). *Environ. Toxicol. Chem.* **2003**, *22* (1), 196−204.
(22) Ahrens, L.; Siebert, U.; Ebinghaus, R. Total body burden and tissue distribution of polyfluorinated compounds in harbor seals (Phoca vitulina) from the German Bight. *Mar. Pollut. Bull.* **2009**, *58* (4), 520−525.
(23) Gannon, S. A.; Johnson, T.; Nabb, D. L.; Serex, T. L.; Buck, R. C.; Loveless, S. E. Absorption, distribution, metabolism, and excretion of [14C]-perfluorohexanoate ([14C]-PFHx) in rats and mice. *Toxicology* **2011**, *283*, 55−62.
(24) Kemper, R. A.; Jepson, G. W. Perfluorooctanoic acid: toxicokinetics in the rat. *Project ID: DuPont* **2003**, 7473.
(25) Chang, S. C.; Noker, P. E.; Gorman, G. S.; Gibson, S. J.; Hart, J. A.; Ehresman, D. J.; Butenhoff, J. L. Comparative pharmacokinetics of perfluorooctanesulfonate (PFOS) in rats, mice, and monkeys. *Reprod. Toxicol.* **2012**, *33* (4), 428−440.
(26) Bogdanska, J.; Sundstrom, M.; Bergstrom, U.; Borg, D.; Abedi-Valugerdi, M.; Bergman, A.; DePierre, J.; Nobel, S. Tissue distribution of 35S-labelled perfluorobutanesulfonic acid in adult mice following dietary exposure for 1−5 days. *Chemosphere* **2014**, *98*, 28−36.
(27) Kelly, B. C.; Ikonomou, M. G.; Blair, J. D.; Surridge, B.; Hoover, D.; Grace, R.; Gobas, F. A. P. C. Perfluoroalkyl contaminants in an Arctic marine food web: Trophic magnification and wildlife exposure. *Environ. Sci. Technol.* **2009**, *43*, 4037−4043.
(28) Gebbink, W. A.; Letcher, R. J. Comparative tissue and body compartment accumulation and maternal transfer to eggs of perfluoroalkyl sulfonates and carboxylates in Great Lakes herring gulls. *Environ. Pollut.* **2012**, *162*, 40−47.
(29) Sharpe, R. L.; Benskin, J. P.; Laarman, A. H.; MacLeod, S. L.; Martin, J. W.; Wong, C. S.; Goss, G. G. Perfluorooctane sulfonate toxicity, isomer-specific accumulation, and maternal transfer in zebrafish (Danio rerio) and rainbow trout (Oncorhynchus mykiss). *Environ. Toxicol. Chem.* **2010**, *29* (9), 1957−1966.
(30) Perez, F.; Nadal, M.; Navarro-Ortega, A.; Fabrega, F.; Domingo, J. L.; Barcelo, D.; Farre, M. Accumulation of perfluoroalkyl substances in human tissues. *Environ. Int.* **2013**, *59*, 354−362.
(31) Han, X.; Nabb, D. L.; Russell, M. H.; Kennedy, G. L.; Rickard, R. W. Renal elimination of perfluorocarboxylates (PFCAs). *Chem. Res. Toxicol.* **2012**, *25* (1), 35−46.
(32) Borg, D.; Lund, B. O.; Lindquist, N. G.; Hakansson, H. Cumulative health risk assessment of 17 perfluoroalkylated and polyfluoroalkylated substances (PFASs) in the Swedish population. *Environ. Int.* **2013**, *59*, 112−123.
(33) Kudo, N.; Sakai, A.; Mitsumoto, A.; Hibino, Y.; Tsuda, T.; Kawashima, Y. Tissue distribution and hepatic subcellular distribution of perfluorooctanoic acid at low dose are different from those at high dose in rats. *Biol. Pharm. Bull.* **2007**, *30* (8), 1535−1540.
(34) Martin, J. W.; Asher, B. J.; Beesoon, S.; Benskin, J. P.; Ross, M. S. PFOS or PreFOS? Are perfluorooctane sulfonate precursors (PreFOS) important determinants of human and environmental perfluorooctane sulfonate (PFOS) exposure? *J. Environ. Monit.* **2010**, *12* (11), 1979−2004.
(35) Aas, C. B.; Fuglei, E.; Herzke, D.; Yoccoz, N. G.; Routti, H. Effect of body condition on tissue distribution of perfluoroalkyl substances (PFASs) in Arctic fox (Vulpes lagopus). *Environ. Sci. Technol.* **2014**, *48* (19), 11654−11661.
(36) Baduel, C.; Lai, F. Y.; Townsend, K.; Mueller, J. F. Size and age−concentration relationships for perfluoroalkyl substances in


DOI: 10.1021/acs.est.7b06128
*Environ. Sci. Technol.* 2018, 52, 4592−4600

stingray livers from eastern Australia. *Sci. Total Environ.* **2014**, *496*, 523−530.
(37) Zhou, Z.; Liang, Y.; Shi, Y.; Xu, L.; Cai, Y. Occurrence and transport of perfluoroalkyl acids (PFAAs), including short-chain PFAAs in Tangxun Lake, China. *Environ. Sci. Technol.* **2013**, *47* (16), 9249−9257.
(38) Shi, Y.; Vestergren, R.; Xu, L.; Song, X.; Niu, X.; Zhang, C.; Cai, Y. Characterizing direct emissions of perfluoroalkyl substances from ongoing fluoropolymer production sources: A spatial trend study of Xiaoqing River, China. *Environ. Pollut.* **2015**, *206*, 104−112.
(39) Shi, Y.; Vestergren, R.; Zhou, Z.; Song, X.; Xu, L.; Liang, Y.; Cai, Y. Tissue Distribution and whole body burden of the chlorinated polyfluoroalkyl ether sulfonic acid F-53B in crucian carp (*Carassius carassius*): Evidence for a highly bioaccumulative contaminant of emerging concern. *Environ. Sci. Technol.* **2015**, *49* (24), 14156−14165.
(40) Karlssonnorrgren, L.; Runn, P. Cadmium dynamics in fish - pulse studies with Cd-109 in female Zebrafish, Brachydanio-Rerio. *J. Fish Biol.* **1985**, *27* (5), 571−581.
(41) Muller, C. E.; De Silva, A. O.; Small, J.; Williamson, M.; Wang, X.; Morrist, A.; Katz, S.; Gamberg, M.; Muir, D. C. G. Biomagnification of perfluorinated compounds in a remote terrestrial food chain: Lichen-caribou-wolf. *Environ. Sci. Technol.* **2011**, *45* (20), 8665−8673.
(42) Martin, J. W.; Mabury, S. A.; Solomon, K. R.; Muir, D. C. Bioconcentration and tissue distribution of perfluorinated acids in rainbow trout (Oncorhynchus mykiss). *Environ. Toxicol. Chem.* **2003**, *22* (1), 196−204.
(43) Houde, M.; De Silva, A. O.; Muir, D. C.; Letcher, R. J. Monitoring of perfluorinated compounds in aquatic biota: an updated review: PFCs in aquatic biota. *Environ. Sci. Technol.* **2011**, *45* (19), 7962−7973.
(44) Jin, H.; Zhang, Y.; Jiang, W.; Zhu, L.; Martin, J. W. Isomer−specific distribution of perfluoroalkyl substances in blood. *Environ. Sci. Technol.* **2016**, *50* (14), 7808−7815.
(45) Hanssen, L.; Dudarev, A. A.; Huber, S.; Odland, J. O.; Nieboer, E.; Sandanger, T. M. Partition of perfluoroalkyl substances (PFASs) in whole blood and plasma, assessed in maternal and umbilical cord samples from inhabitants of arctic Russia and Uzbekistan. *Sci. Total Environ.* **2013**, *447*, 430−437.
(46) Salvalaglio, M.; Muscionico, I.; Cavallotti, C. Determination of energies and sites of binding of PFOA and PFOS to human serum albumin. *J. Phys. Chem. B* **2010**, *114* (46), 14860−14874.
(47) Bischel, H. N.; Macmanus-Spencer, L. A.; Zhang, C. J.; Luthy, R. G. Strong associations of short-chain perfluoroalkyl acids with serum albumin and investigation of binding mechanisms. *Environ. Toxicol. Chem.* **2011**, *30* (11), 2423−2430.
(48) Escher, B. I.; Schwarzenbach, R. P.; Westall, J. C. Evaluation of liposome - water partitioning of organic acids and bases. 1. Development of a sorption model. *Environ. Sci. Technol.* **2000**, *34* (18), 3954−3961.
(49) Zhao, W.; Zitzow, J. D.; Weaver, Y.; Ehresman, D. J.; Chang, S. C.; Butenhoff, J. L.; Hagenbuch, B. Organic anion transporting polypeptides contribute to the disposition of perfluoroalkyl acids in humans and rats. *Toxicol. Sci.* **2016**, *156* (1), 84−95.
(50) Wang, Z. Y.; MacLeod, M.; Cousins, I. T.; Scheringer, M.; Hungerbuhler, K. Using COSMOtherm to predict physicochemical properties of poly- and perfluorinated alkyl substances (PFASs). *Environ. Chem.* **2011**, *8* (4), 389−398.
(51) Weaver, Y. M.; Ehresman, D. J.; Butenhoff, J. L.; Hagenbuch, B. Roles of rat renal organic anion transporters in transporting perfluorinated carboxylates with different chain lengths. *Toxicol. Sci.* **2010**, *113*, 305−314.
(52) Yang, C. H.; Glover, K. P.; Han, X. Characterization of cellular uptake of perfluorooctanoate via organic anion-transporting polypeptide 1A2, organic anion transporter 4, and urate transporter 1 for their potential roles in mediating human renal reabsorption of perfluorocarboxylates. *Toxicol. Sci.* **2010**, *117*, 294−302.
(53) Woodcroft, M. W.; Ellis, D. A.; Rafferty, S. P.; Burns, D. C.; March, R. E.; Stock, N. L.; Trumpour, K. S.; Yee, J.; Munro, K. Experimental characterization of the mechanism of perfluorocarboxylic acids' liver protein bioaccumulation: The key role of the neutral species. *Environ. Toxicol. Chem.* **2010**, *29*, 1669−1677.
(54) Zhang, L.; Ren, X. M.; Guo, L. H. Structure-based investigation on the interaction of perfluorinated compounds with human liver fatty acid binding protein. *Environ. Sci. Technol.* **2013**, *47*, 11293−11301.
(55) MacManus-Spencer, L. A.; Tse, M. L.; Hebert, P. C.; Bischel, H. N.; Luthy, R. G. Binding of perfluorocarboxylates to serum albumin: A comparison of analytical methods. *Anal. Chem.* **2010**, *82*, 974−981.
(56) Bischel, H. N.; Macmanus-Spencer, L. A.; Luthy, R. G. Noncovalent interactions of long-chain perfluoroalkyl acids with serum albumin. *Environ. Sci. Technol.* **2010**, *44*, 5263−5269.
(57) Hebert, P. C.; MacManus-Spencer, L. A. Development of a fluorescence model for the binding of medium- to long-chain perfluoroalkyl acids to human serum albumin through a mechanistic evaluation of spectroscopic evidence. *Anal. Chem.* **2010**, *82*, 6463−6471.
(58) Han, X.; Snow, T. A.; Kemper, R. A.; Jepson, G. W. Binding of perfluorooctanoic acid to rat and human plasma proteins. *Chem. Res. Toxicol.* **2003**, *16*, 775−781.
(59) Chen, Y. M.; Guo, L. H. Fluorescence study on site-specific binding of perfluoroalkyl acids to human serum albumin. *Arch. Toxicol.* **2009**, *83*, 255−261.
(60) Beesoon, S.; Martin, J. W. Isomer-Specific Binding affinity of perfluorooctanesulfonate (PFOS) and perfluorooctanoate (PFOA) to serum proteins. *Environ. Sci. Technol.* **2015**, *49*, 5722−5731.
(61) Liu, C.; Gin, K. Y.; Chang, V. W.; Goh, B. P.; Reinhard, M. Novel perspectives on the bioaccumulation of PFCs–the concentration dependency. *Environ. Sci. Technol.* **2011**, *45*, 9758−9764.


DOI: 10.1021/acs.est.7b06128
*Environ. Sci. Technol.* 2018, 52, 4592−4600